Existence of ponderomotive effects for plane, uniform electromagnetic waves of arbitrary polarisation in a magnetoplasma

By R. Uma and D. Subbarao

Fusion Studies Program, Centre of Energy Studies, Indian Institute of
Technology, New Delhi - 110 016, India

Abstract. The stationary ponderomotive force of an arbitrarily polarised, plane, uniform electromagnetic wave in a magneto-plasma is shown to be space-periodic with the characteristic length of the order of wavelength of the normal modes. The longitudinal part of the force modulates the plasma normal to the boundary for all angles of incidence of the electromagnetic wave. The nonlinear dispersion characteristics as a result show total and partial Bragg reflection for normal and oblique incidence of the wave respectively in the stop (unstable) bands and spatial harmonic generation in the pass (stable) bands.

1. Introduction

The concept of ponderomotive force finds applications in several nonlinear phenomena relevant to laser-plasma interaction [1], heating, r.f. plugging and stabilisation of magnetically confined fusion plasmas [2, 3, 4] and wave propagation in ionosphere [5]. In laser-plasma interaction, the coupling of the pump (laser) to the modes of the plasma through the force leads to parametric instabilities [6], while the density redistribution due to the radiation pressure causes self-focusing of electromagnetic beams [7], anomalous reflection [8] and soliton propagation [9]; the ponderomotive force of finite amplitude electromagnetic and electrostatic waves can help deliver a net momentum to the plasma, generating a zero-frequency current and magnetic field [10].

Several derivations of the ponderomotive force based on Helmholtz method [13], fluid and kinetic picture of the plasma [14, 15], as reviewed in Ref. 16 exist; the most general of these being the Lie-transform formalism due to Cary *et al.* However, with the exception of Refs. 16, 17 and 18, all of these studies consider the ponderomotive force and its effects only for waves with inhomogeneous intensity profiles.

In this paper, we examine an effect for uniform plane waves missed until recently, namely that almost every conceivable system that launches a wave in the plasma, will excite a super-position of waves which having the same frequency ω but different wavenumber k will generate by mixing, a zero frequency spatial

periodic structure. This structure then influences the propagation of the wave, resulting in new ponderomotive effects like nonlinear Bragg reflection in the stop bands and spatial harmonic generation in the pass bands.

The above ponderomotive effects are studied in detail in the high frequency regime in a cold, unbounded, magnetoplasma, where for a given ω, two characteristic modes with different polarisations propagate (note that these waves can no longer be termed 'modes' as they cease to be independent in the nonlinear regime). While this is the first such study for unbounded systems interacting with an external electromagnetic energy source, the above effects could also arise in bounded systems where oppositely propagating waves that constitute an eigen-mode beat to give zerofrequency modification on the ponderomotive force. Examples of the latter are the excitation of cavity modes investigated recently by Festeau *et al.* [12] in the ioncyclotron regime in a two-species plasma and the earlier studies on radio frequency confinement [11] and other effects such as self-focusing [7].

The organisation of the paper is as follows: Section 2 gives expressions for the longitudinal and solenoidal part of the ponderomotive force for normal incidence and the resulting density redistribution while Section 3 deals with the wave equation in the modulated plasma and the nature of the solutions in the stable and unstable regions. Section 4 is devoted to the phenomena of nonlinear Bragg reflection. Finally Section 5 gives a summary of results, applications and conclusions.

2. The stationary ponderomotive force density and density redistribution

We define the ponderomotive force density as the time independent force density obtained by averaging all the nonlinearities in the first moment of the Vlasov equation over the fast time scale (16, 17)

$$\mathbf{F}_{p\alpha} = \left\langle \rho_\alpha \mathbf{E} + \frac{1}{c} \mathbf{J}_\alpha \times \mathbf{B} \right\rangle - \frac{4\pi}{\omega_{p\alpha}^2} \left\langle \mathbf{\nabla} \cdot \mathbf{J}_\alpha \mathbf{J}_\alpha \right\rangle \tag{1}$$

where α refers to the charge species, ρ_α and $\mathbf{J}_\alpha$ are the charge and current densities respectively. $\omega_{p\alpha} = (4\pi n_{0\alpha} e^2 / m_{0\alpha})^{1/2}$ is the characteristic plasma frequency, $n_{0\alpha}$ and m_α are the number density and mass respectively; e is the electronic charge, c is the speed of light in vacuum, c.c. refers to complex conjugate. This definition more accessible for uniform plane waves [18], generalises the definition in terms of a gradient force [20] which is applicable to inhomogeneous fields.

The linear high frequency response of the cold magnetoplasma in the presence of an incident wave of frequency ω can, in general, be expressed as a superposition of the two normal waves of different wavenumbers and polarisation. We have, in mind in this paper, the region of propagation of fast extraordinary (FE) and ordinary (O) waves; that of ordinary and slow extraordinary (SE) waves; and fast magnetosonic (FMS) and slow extraordinary (SE) waves. External pumping of a plasma is also possible in other frequency regimes

such as that of Alfven waves where the analysis should essentially be the same. With

$$\mathbf{E} = \sum_\alpha E_\alpha \hat{\mathbf{e}}_\alpha \exp\left(i(-\mathbf{K}_\alpha \cdot \mathbf{r} + \omega t)\right) \qquad \alpha = 1, 2 \tag{2a}$$

E_α being the complex amplitudes and $\hat{\mathbf{e}}_\alpha$ the normalised eigenvectors corresponding to the two normal modes and use of the continuity and Maxwell's equations, we get

$$\rho \mathbf{E}^* = \frac{1}{\omega} \sum_{\alpha,\beta} (\mathbf{K}_\alpha \cdot \boldsymbol{\sigma} \cdot \mathbf{E}_\alpha)\mathbf{E}_\beta^* \tag{2b}$$

$$\frac{1}{c}(\mathbf{J} \times \mathbf{B}^*) = \frac{1}{\omega} \sum_{\alpha,\beta} [\mathbf{K}_\beta(\boldsymbol{\sigma} \cdot \mathbf{E}_\alpha \cdot \mathbf{E}_\beta^*) - \mathbf{E}_\beta^*(\mathbf{K}_\beta \cdot \boldsymbol{\sigma} \cdot \mathbf{E}_\alpha)] \tag{2c}$$

where $\alpha = 1, 2$ and $\beta = 1, 2$.

Equations (2b) and (2c) may then be simplified by the use of $\nabla \cdot \mathbf{D} = 0$ and the orthogonality relations between the normal modes [19],

$$\mathbf{K}_\alpha \cdot \boldsymbol{\sigma} \cdot \mathbf{E}_\alpha = -\frac{i\omega}{4\pi}(\mathbf{K}_\alpha \cdot \mathbf{E}_\alpha) \tag{2d}$$

$$(\delta_{ij} - \hat{K}_i \hat{K}_j)\hat{e}_{i\beta}^* \hat{e}_{j\alpha} = \delta_{\alpha\beta} \tag{2e}$$

where $\hat{K}_i$, $\hat{K}_j$ are the components of the unit propagation vector. More conveniently, equation (2e) on substitution in the equation for $\hat{e}_{j\alpha}$ i.e.

$$(N_\alpha^2(\delta_{ij} - K_i K_j) - \epsilon_{ij}(N_\alpha, \omega))\hat{e}_{j\alpha} = 0 \tag{2f}$$

gives

$$\epsilon_{ij}\hat{e}_{j\alpha}\hat{e}_{i\beta}^* = N_\alpha^2 \delta_{\alpha\beta} \tag{2g}$$

where N_α is the refractive index of the αth mode and ϵ_{ij} refers to the dielectric tensor $(\epsilon_{ij} = 1 - 4\pi i \sigma_{ij}/\omega)$.

Equation (2g) shows that the eigenvectors are not mutually orthogonal as they are not purely transverse or longitudinal as in an isotropic plasma; their transverse components are, however, mutually orthogonal. Equation (2g) also implies

$$\begin{aligned}
\boldsymbol{\sigma}/\omega \cdot \mathbf{E}_\alpha \cdot \mathbf{E}_\beta^* &= -iE_\alpha E_\beta(1 - N_\alpha^2)/4\pi & \alpha = \beta \\
&= -i\mathbf{E}_\alpha \cdot \mathbf{E}_\beta^*/\overline{4\pi} & \alpha \neq \beta
\end{aligned} \tag{2h}$$

so that equations (2b) and (2c) become

$$\rho \mathbf{E}^* + \frac{1}{c}(\mathbf{J} + \mathbf{B}^*) + \text{c.c.} = \sum_{\substack{\alpha,\beta \\ \alpha \neq \beta}} \left[\frac{i}{4\pi}(\mathbf{K}_\alpha(\mathbf{E}_\beta \cdot \mathbf{E}_\alpha^*) - (\mathbf{K}_\alpha - \mathbf{K}_\beta) \cdot \mathbf{E}_\alpha \mathbf{E}_\beta^*) \right] + \text{c.c.} \tag{2i}$$

while

$$\nabla \cdot \mathbf{J}\mathbf{J}^* = \frac{i\omega^2}{16\pi^2} \sum_{\alpha,\beta} (\mathbf{K}_\alpha - \mathbf{K}_\beta) \cdot \mathbf{E}_\alpha(\mathbf{D}_\beta^* - \mathbf{E}_\beta^*) \tag{2j}$$

Equation (1) can be written using equations (2d) and (2h) as

$$\mathbf{F}_p = \frac{i}{16\pi} \{ (\mathbf{K}_1 - \mathbf{K}_2) \cdot [I(\mathbf{E}_1 \cdot \mathbf{E}_2^*) - \omega^2/\omega_p^2(\mathbf{E}_1 \mathbf{D}_2^* - \mathbf{E}_2 \mathbf{D}_1^*)$$

$$- (1 - \omega^2/\omega_p^2)(\mathbf{E}_2 \mathbf{E}_2^* - \mathbf{E}_2 \mathbf{E}_1^*)]\} + \text{c.c.} \tag{3a}$$

The ponderomotive force hence vanishes for propagation of the characteristic waves parallel to the magnetic field and can be seen to be periodic in space with the characteristic length $|\mathbf{K}_1 - \mathbf{K}_2|^{-1}$.

One may separate the longitudinal part of $\mathbf{F}_p$ which can be expressed as a gradient of a scalar. This component is parallel to $(\mathbf{K}_1 - \mathbf{K}_2)$ and is denoted by $\mathbf{F}_{p\parallel}$ below:

$$\mathbf{F}_{p\parallel} = (\mathbf{K}_1 - \mathbf{K}_2)E_{1z}E_{2z}^*(2\omega^2/\omega_p^2 - 1) \sin ((K_1 - K_2)z)/8\pi \tag{3b}$$

where (21)

$$E_{1z}E_{2z}^* = E_1 E_2 \frac{\epsilon_2(\epsilon_3 - N_1^2)(\epsilon_3 - N_2^2) \sin^2 \theta}{\epsilon_3(N_2^2 - N_1^2)(\epsilon_1 \sin^2 \theta + \epsilon_3 \cos^2 \theta)} \tag{3c}$$

With

$$\epsilon_1 = 1 + \frac{\omega_{pe}^2}{(\omega_{ce}^2 - \omega^2)}, \qquad \epsilon_2 = \frac{\omega_{ce}}{\omega} \frac{\omega_{pe}^2}{(\omega_{ce}^2 - \omega^2)}, \qquad \epsilon_3 = 1 - \frac{\omega_{pe}^2}{\omega^2},$$

ω_{ce} being the electron cyclotron frequency, θ the angle of propagation of the modes with respect to the magnetic field. Equation (3b) vanishes both for wave propagation along and perpendicular to the magnetic field $\boldsymbol{B}_0$. This might be one of the reasons for its not having been investigated till now; Fig. 1 gives the
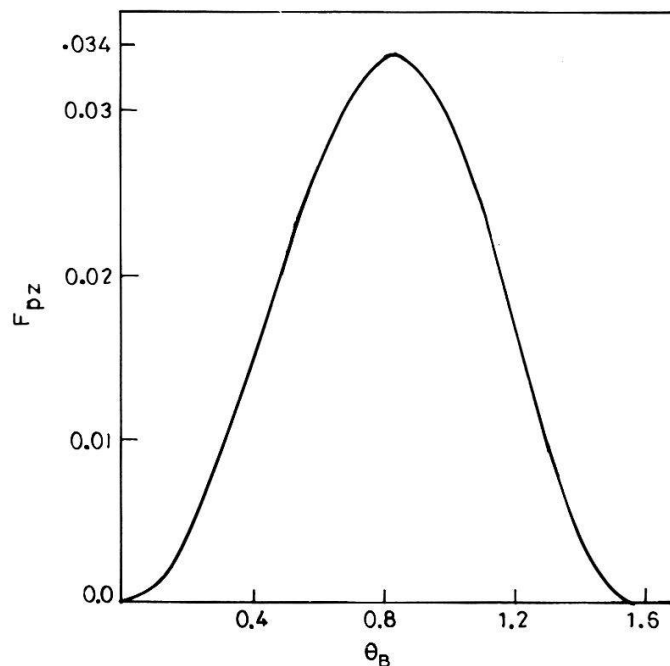

Figure 1
The nonsolenoidal component of the ponderomotive force ($\mathrm{F}_{p\parallel}$) vs. the angle of propagation (θ_B) of the linear modes with respect to the magnetic field, for normal incidence.

estimates of the force for intermediate angles of propagation (with respect to the magnetic field direction).

The solenoidal part of equation (3a) can be written as

$$\mathbf{F}_{p\perp} = -\frac{(K_1 - K_2)}{8\pi} \frac{1}{(\epsilon_1 \sin^2 \theta + \epsilon_3 \cos^2 \theta)} (F_{px} \sin((K_1 - K_2)z)\hat{\mathbf{x}}$$

$$+ F_{py} \cos((K_1 - K_2)z)\hat{\mathbf{y}})$$

where

$$F_{px} = \frac{\epsilon_2 \sin \theta}{N_2^2 - N_1^2} \{(1 - \omega^2/\omega_p^2)(2\epsilon_3 - (N_1^2 + N_2^2))$$

$$+ \omega^2/\omega_p^2(\epsilon_3(N_1^2 + N_2^2) - 2N_1^2 N_2^2)\}$$

$$F_{py} = (\epsilon_1 \sin^2 \theta + \epsilon_3 \cos^2 \theta) \sin \theta \left\{ (1 - \omega^2/\omega_p^2) \right.$$

$$\left. \times \frac{\epsilon_3 - \epsilon_1}{N_2^2 - N_1^2} \cos^2 \theta + \frac{\omega^2}{\omega_p^2} ((N_1^2 + N_2^2) - \epsilon_1\epsilon_3 - N_1^2 N_2^2/\epsilon_3) \right\} \tag{3d}$$

In this paper we do not take up the current and magnetic field generation by $\mathbf{F}_{p\perp}$. It may also be noted that the orthogonality relations (equations (2h)) used to obtain the ponderomotive force above (equation (3)) apply when the two characteristic waves propagate at the same angle to the magnetic field. To see when such collinear propagation of the two waves occurs, consider the electromagnetic wave to be incident at an angle θ_{in} with respect to the normal ($\hat{z}$) to the vacuum-plasma interface, with the magnetic field at an angle θ_B (different in general from θ defined earlier) with respect to the z direction such that

$$\sin \theta_{in} = N_1 \sin \theta_1 = N_2 \sin \theta_2 \tag{4a}$$

and

$$(\mathbf{K}_1 - \mathbf{K}_2) \cdot \mathbf{r} = 0 \tag{4b}$$

from continuity of the fields across the boundary. Here θ_1 and θ_2 are the angles of propagation of the two modes with respect to the normal and N_1, N_2 are the refractive indices of the two modes evaluated at $(\theta_1 - \theta_B)$ and $(\theta_2 - \theta_B)$ respectively; $\mathbf{r}$ is a vector along the vaccum-plasma boundary and is in the y direction so that $(\mathbf{K}_1 - \mathbf{K}_2)$ is along the normal (see equation (4b)). From equation (4a), it is clear that the two characteristic waves propagate collinearly for normal incidence ($\theta_1 = \theta_2 = \theta_{in} = 0$), the magnetic field being at an arbitrary angle $\theta_B(=\theta)$ with respect to the direction of propagation of the normal waves.

For oblique incidence, the two normal waves propagate non-collinearly ($\theta_1 \neq \theta_2$). The ponderomotive force may then still be expressed as

$$\mathbf{F} = \mathbf{F}_{p0} \exp(i(K_1 - K_2)z) + \text{c.c.} \tag{5}$$

from equations (1) and (4). An explicit expression can be obtained for $\mathbf{F}_{p0}$ along the lines of equations (2) and (3) and is not gone into, as it is not relevant to the

ponderomotive effects considered here. However, the basic consequences are still discernible; we come to this aspect again in Section 4 (equations (14)).

Density modulation

Though we consider a two-species electron-ion plasma, the contribution of ions in the linear dielectic constant may be ignored when $\omega^2 \gg \omega_{ci}\omega_{ce}$; the ponderomotive force on the ions is also negligible as the force varies inversely as the mass of the species. While the latter is not explicit in the expressions (3c) and (3d) it can, for example, be easily verified for quasilongitudinal and quasitransverse propagation.

In steady state, an electric field consistent with the nonsolenoidal part of the ponderomotive force (acting on the electrons) develops, which is balanced by the thermal drag on the ions (The ions follow the electrons) i.e.

$$\mathbf{E}_{s\|} = K_B T_e / e \nabla \delta n_i / n_0 \tag{6a}$$

From equation (4a), the electron momentum equation

$$0 = \mathbf{F}_{p\|} - e\mathbf{E}_{s\|} - K_B T_e \nabla \delta n_e / n_0 \tag{6b}$$

and the assumption of quasineutrality, (which persists as the scalelength of the potential is much greater than the Debye length) the selfconsistent modulation due to the longitudinal ponderomotive force may be determined [19]; it is along the normal to the vacuum-plasma boundary irrespective of the angle of incidence of the electromagnetic wave, as can be seen from equation (4). For normal incidence, it is given by

$$\frac{\delta n}{n} = \frac{(1 - 2\omega^2/\omega_p^2)}{n_0(T_e + T_i)} E_{1z} E_{2z}^* (\cos (K_1 - K_2)z - 1)/8\pi \tag{6c}$$

This zero frequency modulation vanishes when the two modes propagate parallel or perpendicular to the magnetic field just as the longitudinal ponderomotive force does.

3. Wave equation and its solutions

Assuming $\mathbf{E} = E_1 \hat{\mathbf{e}}_1 + E_2 \hat{\mathbf{e}}_2$ to still hold in the modulated plasma, (henceforth called the parametric approximation in this paper) a steady state solution for E_1 and E_2 can be obtained after incorporating the self-induced density modification in the wave equation of each of the normal modes. In this parametric approximation, when $\delta N_\alpha \ll N_\alpha$, N_α being the perturbation in the refractive index for the α-th mode corresponding to the density perturbation δn, i.e.

$$N_\alpha^2(n) = N_\alpha^2(n_0) + \left.\frac{\partial N_\alpha^2}{\partial n}\right|_{n=n_0} \delta n + \cdots \tag{7}$$

the nonlinearity is weak and is calculated using unmodified eigenmodes. In the

same approximation, the selfgenerated currents and associated magnetic fields have negligible effect on wave propagation [22].

Let us first consider the case of normal incidence, where $\delta n/n$ is given by equation (6c). The propagation of the eigenmodes is governed in the present approximation by the Mathieu equation [23],

$$\frac{d^2 E_{1,2}}{d\bar{z}^2} + (a_{1,2} - 2q_{1,2} \cos 2\bar{z})E_{1,2} = 0$$

where

$$\bar{z} = (K_1 - K_2)z/2, \qquad a_{1,2} = 4N_{1,2}^2/(N_1 - N_2)^2 \tag{8}$$

$$q_{1,2} = -\left(\frac{\partial N_{1,2}^2}{\partial n}\right)(1 - 2\omega^2/\omega_p^2)\frac{E_{1z}E_{2z}^*}{2\pi(T_e + T_i)}\frac{1}{(N_1 - N_2)^2}$$

and $|q/a| \ll 1$.

As dictated by the Mathieu stability diagram, periodic and aperiodic but bounded solutions can be constructed in the stable region (pass bands) while the unstable regions (stop bands) situated near $a \simeq m^2$, $m = 0, 1, 2, \ldots$, allow growing (unbounded) solutions and decaying (evanescent) solutions in space. We consider only decaying solutions in the unstable band; the growing solution is unphysical in the semi-infinite, passive medium which has no free energy to amplify the wave. However, the modulated medium can act as an active medium for a small amplitude test wave which satisfies the Bragg (stop band) condition. This could lead to spatial amplification of the test wave as in parametric amplifiers [25] and is not taken up here.

Consider the Floquet solution of equation (8),

$$E(\bar{z}) \simeq A \exp(-\mu\bar{z})\Phi(\bar{z}, \sigma) \tag{9}$$

where $\Phi(\bar{z}, \sigma)$ is a periodic function of $\bar{z}$. In the stable and unstable region between A_1 and B_2 (Fig. 2) it is given by

$$\Phi(\bar{z}, \sigma) \simeq (\exp(i\bar{z}) + R_1 \exp(-i\bar{z}) + A_3(\exp(i3\bar{z}) + R_3 \exp(-i3\bar{z})) + \cdots$$

where

$$R_1 = \exp(i2\sigma); \qquad R_3 = \left(\frac{c_3 + is_3}{c_3 - is_3}\right)\exp(i6\sigma);$$

$$A_3 = i(c_3 - is_3)\exp(i2\sigma) \tag{9a}$$

Here σ and δ are complex parameters dependent on a and q and are given by

$$\sigma = \tfrac{1}{2}\arccos\delta; \qquad \mu = q/2(1 - \delta^2)^{1/2};$$

$$\delta = \frac{2}{q}[1 - (a + \tfrac{3}{8}q^2)^{1/2}]$$

$$s_3 = -q/8 + q^2 \cos 2\sigma/64 + \cdots$$

$$c_3 = \tfrac{3}{64}q^2 \sin 2\sigma - \tfrac{3}{512}q^3 \sin 4\sigma + \cdots \tag{9b}$$
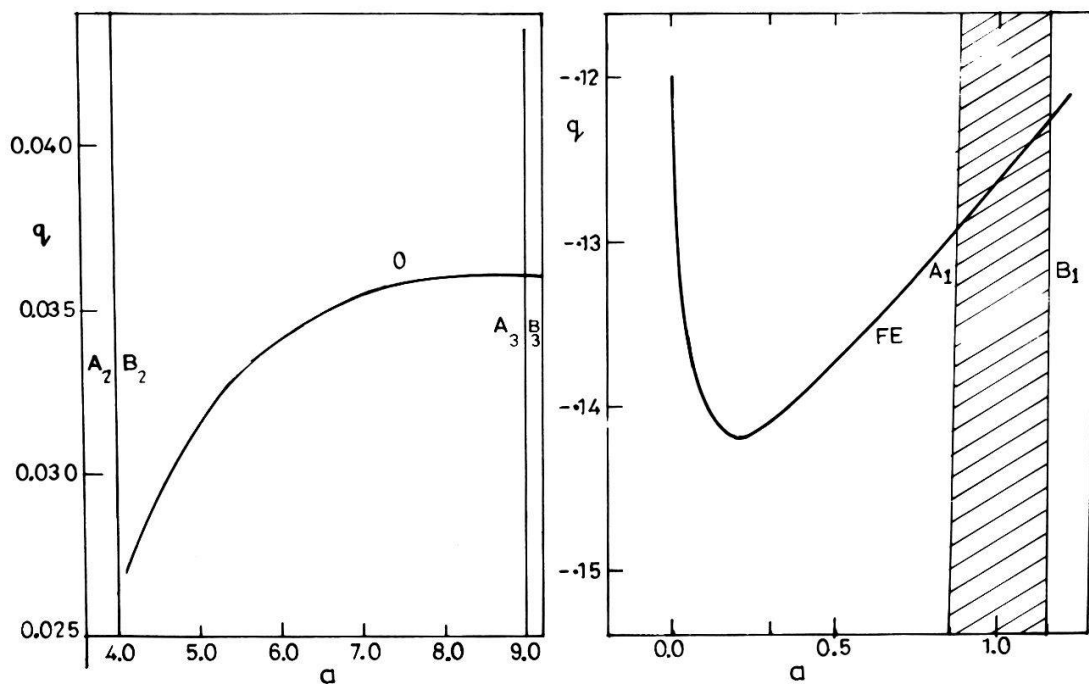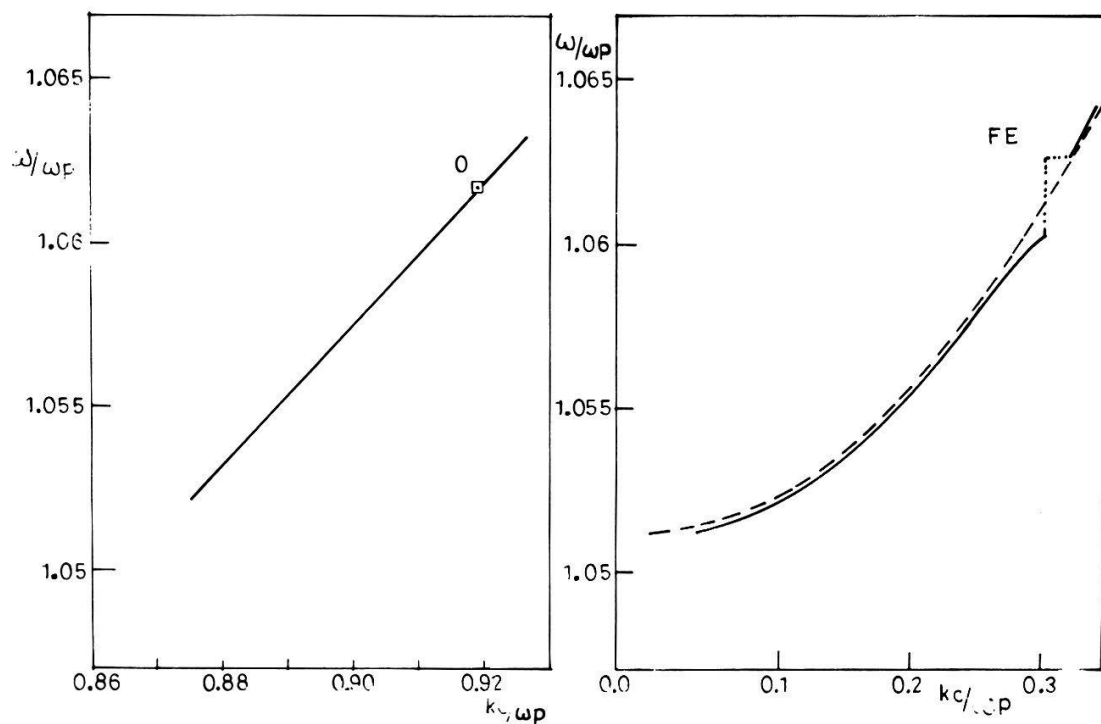
Figure 2(a)

Figure 2(b)

Figure 2

The high frequency region of the magneto-plasma with $\omega > \omega_{pe} \gg \omega_{ce}$ and $\theta_B = 10°$ for normal incidence. (a) The stability diagram for the Mathieu equation superimposed by the curves $a(\omega)$ and $q(\omega)$ (ω increases towards the right on the curves) corresponding to FE and O Waves: with $\omega_e/\omega_p = 0.1$; (b) Dispersion curve (Brillouin Diagram) derived from (a). Continuous curve – nonlinear and dotted – linear.

In the stable (pass) bands, μ is imaginary and $|R_1|$ and $|R_3|$ in (equation (9a)) decay to zero some distance from the boundary of the stop band. The wave can propagate in this region. It, however, excites a spectrum of sidebands at different wavenumbers though at the same frequency. For example, the solution in the pass band between A_1, B_2, with $\mu = i(1 + \beta)$ and $0 < \beta < 1$, is described in terms of Mathieu functions of real fractional order viz $Ce_{1+\beta}(a, q)$ and $Se_{1+\beta}(a, q)$

$$E(\bar{z}) \simeq \exp\left(i(1 + \beta)\bar{z}\right) - \frac{q}{4}\left[\frac{\exp\left(i(3 + \beta)\bar{z}\right)}{3 + \beta} - \frac{\exp\left(i(\beta - 1)\bar{z}\right)}{\beta - 1}\right] + \cdots \qquad (10)$$

This solution is periodic when β is rational and is aperiodic but bounded when β is irrational. The solution shows that the primary wave with wavenumber $(\beta + 1)$ is coupled to sidebands of higher wavenumbers $(\beta + 1 \pm n)$ through the modulation of strength q. Considering the coupling only to the sidebands $n = \pm 1$ to be significant, the dispersion relation for the wave may be written as

$$K \simeq (K_1 - K_2)(1 + \beta) \simeq (K_1 - K_2)\left(a - \frac{a - 1}{2(a - 1)^2 - q^2}q^2\right.$$

$$\left. - \frac{5a + 7}{32(a - 1)^3(a - 4)}q^4\right)^{1/2} \qquad (11)$$

under the approximation $|a| \gg |q^2/(1 + \beta)^2 - 1|$.

The existence of coupling to sidebands with higher wavenumbers (lower phasevelocities) suggests the possibility of enhancement in wave damping [22].

In the unstable bands, μ is real while it is zero on the boundary A_1, B_1 for the first band near $a \simeq 1$ in Fig. 2. The width of these bands depends on the strength of the modulation; for example, near $a \simeq 1$, the width of the stop band is q/a and given by the condition $1 - q/2a < a < 1 + q/2a$. On the boundary A_1 and B_1, the solution corresponds to the integral Mathieu functions $Se_1(a, q)$ and $Ce_1(a, q)$. Here the harmonics couple exactly in pairs and correspond to purely standing waves. Inside the stop band, the solution equation (9) gives a superposition of standing waves exponentially damped in the z direction. This implies that the mode considered is evanescent in the plasma in the stop bands; accordingly the component of the electromagnetic wave with the polarisation of the evanescent mode is Bragg reflected.

The case of oblique incidence could be analysed likewise. With $E_\alpha = E_{0\alpha} \exp{(ik_y\bar{y})}Z_i(\bar{z})$; $\alpha = 1, 2$, one may write down a Mathieu equation from equation (4) as in equation (9) for $Z_i(\bar{z})$ with $a_\alpha^2 = 4(K_\alpha^2 - K_0^2 \sin^2 \theta_{in})/(K_1 - K_2)^2$ where K_α^2 ($\alpha = 1, 2$) are evaluated at the angle of propagation $\theta_B - \theta_\alpha$, θ_B being the angle made by the magnetic field with the normal. The stopband condition then becomes

$$4(N_\alpha^2 - N_0^2 \sin^2 \theta_{in})/(N_1 - N_2)^2|_{\theta_B - \theta_\alpha} = m^2 \qquad (12)$$

The significance of (12) and details of Bragg reflection are discussed in the next section.

R. Uma und D. Subbarao   H. P. A.

One would observe that the above treatment based on parametric approximation assumes the modulation (of strength q) to be unaffected by the changes in the dispersion characteristics of the modes induced by the nonlinearity. For example, at oblique incidence when one polarisation component of the electromagnetic wave is reflected in the stop band, the evanescent nature of the mode in the plasma would self consistently cause the modulation to decay in space with a period $(q |K_1 - K_2|^{-1})$ (in the first stop band). Besides, the inhomogeneity would give rise to a space dependence in the wave number thereby affecting the Bragg condition. It may therefore appear that the eigenmode solutions (equation (9)) could only apply to a small amplitude test wave which probes the modulation created by the original finite amplitude wave and essentially leaves it undisturbed. However, this is not the case considered and our aim is to develop a selfconsistent description of steadystate nonlinear propagation of the finite amplitude wave in a future communication. While the parametric approximation, in general, should be replaced by a fully selfconsistent analysis, it is shown, below that the above approach is selfconsistent within this approximation and brings out the principal qualitative changes in the propagation characteristics.

To see that the phase coherence between the wave and the modulation is not disturbed in the presence of the evanescent wave (the incident wave is partially Bragg reflected) one may note that the amplitude of the modulation q varies much slowly compared with the phase (i.e. $q |\mathbf{K}_1 - \mathbf{K}_2| \ll |\mathbf{K}_1 - \mathbf{K}_2|$) so that the Mathieu equation for a homogeneous, semi-infinite plasma is locally valid. Hence the maximum value of the changed wave number, given that the unperturbed value is $K_{10} = \frac{1}{2}(K_{10} - K_{20})\sqrt{a_1}$ is $K_1 = \frac{1}{2}(K_1 - K_2)\sqrt{a_1 + q}$ so that $4K_1^2/(K_1 - K_2)^2 = a + q$. Hence the mode remains within the stop band and the Bragg condition continues to be satisfied in spite of q decreasing with z along with the width of the stop band. The parametric assumption involving the scenario of unmodified linear eigenmodes is, therefore, valid. Further if the reflected wave be considered in the determination of the ponderomotive force, a modulation would be created at $\mathbf{K}_1 + \mathbf{K}_2$. This modulation, however, is nonresonant with the wave in the Bragg sense and would, therefore, lead to higher spatial harmonic generation as in the pass bands (equation (10)); it is a higher order effect. Hence considerable Bragg reflection would occur from the fairly large coherent volume before selfconsistent effects (pump depletion) become important.

4. Nonlinear Bragg reflection (NBR)

From the previous section, we found that Bragg reflection of a characteristic wave occurs in the stop band when the scalelength of the ponderomotive induced modulation is an integral multiple of its wavelength. If both the characteristic waves simultaneously satisfy the Bragg condition, the reflection of an arbitrarily polarised electromagnetic wave is total as it is a superposition of the two characteristic waves. For the case of normal incidence, it is easy to see that if the

stop band condition is satisfied by mode 1 i.e.

$$a_1 = 4N_1^2/(N_1 - N_2)^2 = m^2 \qquad m = 0, 1, 2, \ldots \tag{13a}$$

mode 2 also satisfies a similar condition simultaneously i.e.

$$a_2 = 4N_2^2/(N_1 - N_2)^2 = (m \pm 2)^2 \tag{13b}$$

This implies total reflection of the electromagnetic wave occurs in the stop bands at normal incidence.

To identify the Bragg zone given by the stop-band condition, one may note that the refractive indices N_1, N_2 are functions of θ_{in}, $\theta_\alpha - \theta_B, \alpha = 1, 2$ (the latter being the angle of propagation of the modes with respect to the magnetic field) and the plasma parameters ω, ω_p and ω_c. For normal incidence $\theta_{in} = \theta_1 = \theta_2 = 0$ so that for a given ω_c and ω_p equations (13) gives a critical frequency ω (Bragg) and q/a gives the frequency bandwidth about ω (Bragg) at which total NBR would occur. Fig. 2 illustrates the Bragg zones for the (high frequency) region of propagation of the fast extraordinary (FE) and ordinary (O) waves where $\omega > \omega_0^{(1)} > \omega_0^{(2)}$; $\omega_0^{(1)}$, $\omega_0^{(2)}$ are the cut-offs for FE and O respectively. In the stability ('a' VS 'q') diagram (see Fig. 2(a)) the stop bands are shown shaded and are bound by the characteristic curves A_m, B_m ($m = 1, 2$). (If the bands are too narrow, they are indicated by straight lines). Also a plot of $a(\omega)$ VS. $q(\omega)$ for FE and O drawn for monotonically increasing ω is superimposed on this stability diagram; ω_c/ω_p is held fixed and is given by 0.1 in Fig. (2a). Note that this plot satisfies equations (12) and (13); for instance when $a_0 \simeq 9$, $a_{FE} \simeq 1$. In Fig. (2b) the dispersion curve (corresponding to the $a(\omega)$ VS. $q(\omega)$ curve in Fig. (2a)) is plotted using equation (11) for FE and O; the band gaps give the ω's for which $a(\omega)$ lies in the stop band (i.e. $a \simeq m^2$) in the stability diagram. Consider the example of laboratory plasma with $\omega_c/\omega_p \simeq 0.1$ and $\omega_p = 1\text{GHZ}$. One may infer from Fig. (2) that the critical Bragg frequency ω (Bragg) $= 1.00617\,\text{GHz}$ with the stop band gap $\Delta\omega \simeq 0.5 \times 10^2\,\text{HZ}$ at normalised power of the wave $E^2/8\pi n_0 T_e \simeq 10^{-3}$. Similarly for ionosphere ω (Bragg) $= 1.00617 \times 10^7\,\text{Hz}$ and $\Delta\omega = 0.5 \times 10^2$. Hz at $E^2/8\pi n_0 T_e = 0.1$, $\omega_p = 10^7\,\text{Hz}$.

The stop bands are pronounced at lower order resonances and are narrowed for higher order resonances. If too narrow, they are shown by a dotted square in the dispersion curve. In the pass bands also, the deviation of kc/ω_p from the linear mode number becomes small in that case.

Figure 3 considers the case of the low density plasma when three frequency regimes are accessible for both the linear modes simultaneously. The first region is that of FE and O considered in Fig. 2 and is not plotted. The second region lies between $\omega_0^{(2)} < \omega < \omega_\infty^{(1)}$ where the slow extraordinary (SE) and ordinary (O) waves propagate (Fig. (3a) and (3b)). The third region of propagation is that of fast magnetosonic (FMS) and the slow extraordinary (SE) waves when $\omega_0^{(3)} < \omega < \omega_\infty^{(2)}$ (Fig. (3c) and (3d)). $\omega_0^{(2)}$, $\omega_0^{(3)}$ are the cut-offs of O and SE while $\omega_\infty^{(1)}$, $\omega_\infty^{(2)}$ are the resonances of FE and SE.

Table 1 gives the normalised critical Bragg frequency ω (Bragg) (for which both the modes are in the stop bands) from Fig. 2 and 3 along with the order of
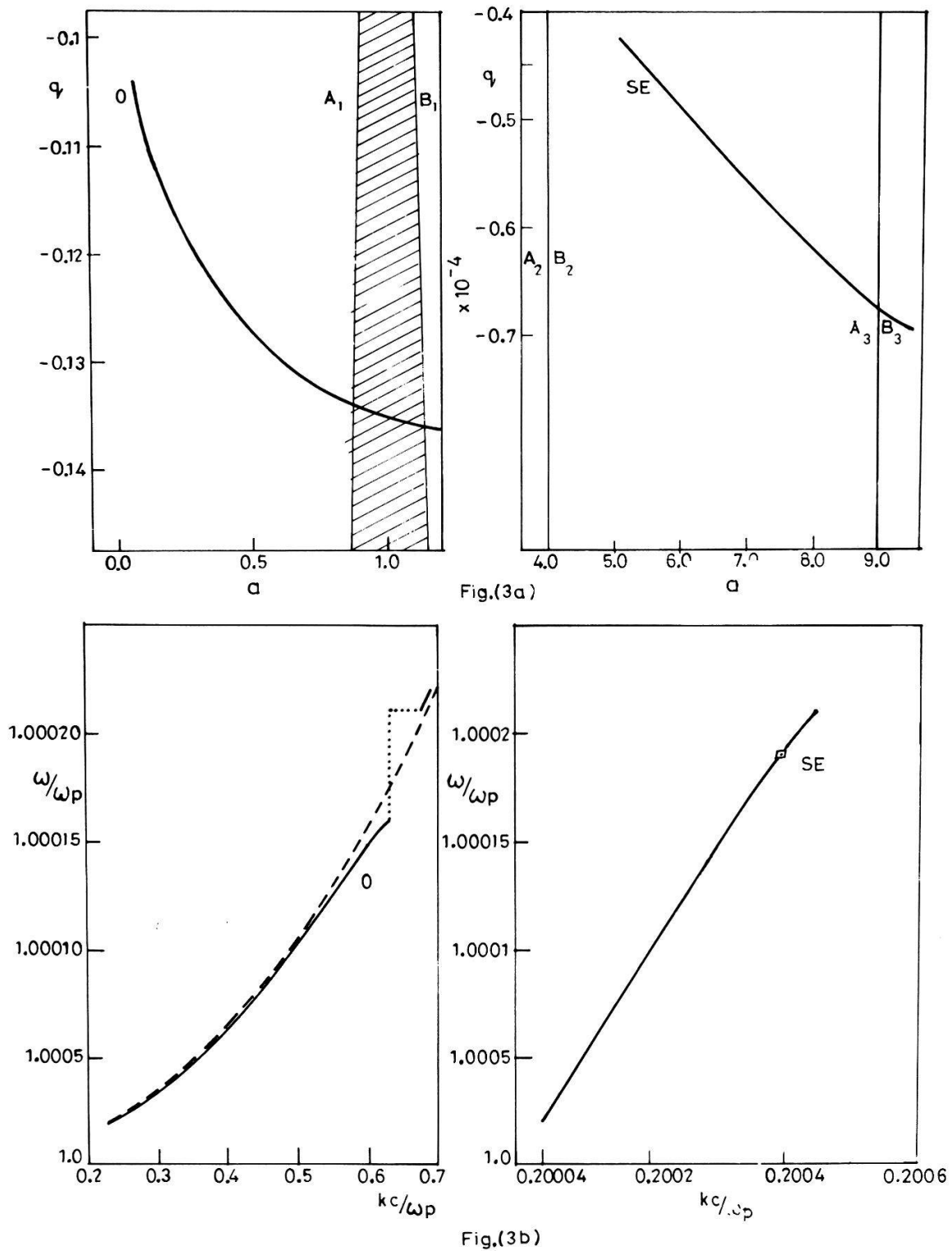
Fig.(3a)

Fig.(3b)

Figure 3

Low density plasma $(\omega_c \gg \omega_p)$ with $\theta_B = 10°$, for normal incidence. The Mathieu stability chart superimposed by the curves $a(\omega)$ and $q(\omega)$ respectively corresponding to (a) SE and O waves for $\omega_0^{(2)} < \omega < \omega_x^{(1)}$ and (c) FMS and SE for $\omega_0^{(3)} < \omega < \omega_x^{(2)}$; (b) and (d). The dispersion curves derived from (a) and (c) respectively. O, FE, SE and FMS correspond to ordinary, slow extraordinary and fast magnetosonic waves respectively.
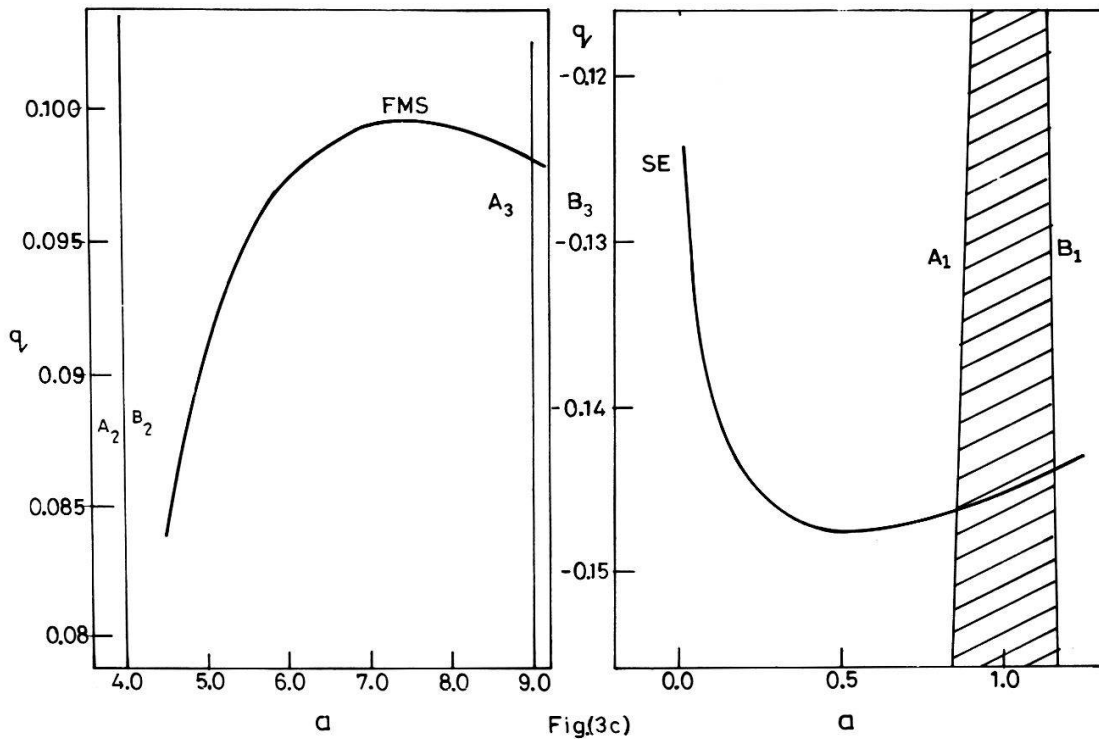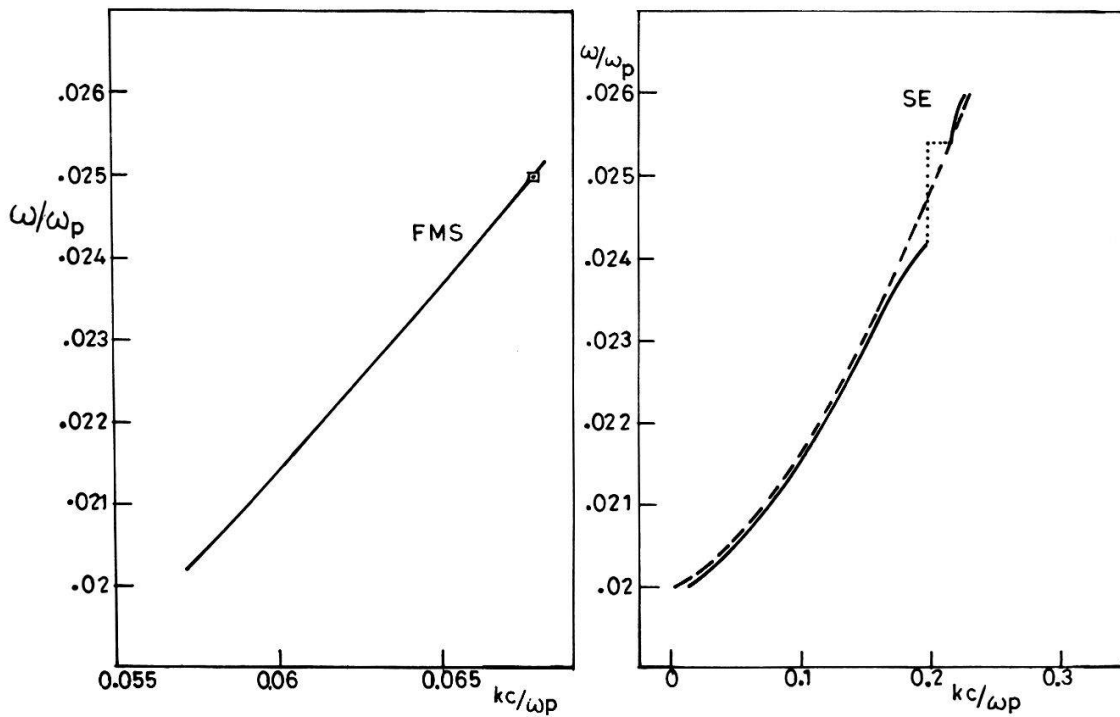
Fig.(3c)

Fig.(3d)

the stop bands. It may be noted that as the frequency band gaps of the two modes are of different widths (as they are of different order) total reflection would occur only in the frequency band common to both the modes; partial reflection would occur in the rest of the stop band corresponding to the mode with the lower order resonance.

Table 1

Normalised Bragg frequency for which the two characteristic waves are in the stop bands ($a_i = 4N_i^2/(N_1 - N_2)^2 = m^2$; $m = 1,3$) for a low density and high density plasma.

ω_c/ω_p	ω/ω_p (Bragg)	Modes (1 & 2)	a_1	a_2
0.01	1.00621	O, FE	9	1
0.1	1.00618	O, FE	9	1
50	1.000175	O, SE	1	9
50	0.025	FMS, SE	9	1

Bragg zones may similarly be determined for the case of oblique incidence of the electromagnetic wave. Here for a given θ_B and plasma parameters ω, ω_p and ω_c the stop band condition in equation (12) defines a certain critical angle of incidence θ_{in} (Bragg) at which reflection would occur. It is convenient to analyse equation (12) as a set of two simpler conditions. N_1^2 can be eliminated using Snell's law to obtain

$$4 \cos^2 \theta_1 = m^2(1 - \sin \theta_1/\sin \theta_2)^2 \tag{14a}$$

The Bragg condition at oblique incidence is therefore equivalent to equation (14a) & Snell's law viz.

$$N_1 \sin \theta_1 = N_2 \sin \theta_2 = \sin \theta_{in} \tag{14b}$$

Table 2 given the values of θ_{in} (Bragg) calculated numerically by optimising the values of ω, ω_p and ω_c simultaneously to satisfy equations (14a) and (14b). For the case of laboratory plasma (or ionosphere as considered in the earlier example) with $\omega_c/\omega_p = 0.13$, one may infer that at θ_{in} (Bragg) $= 0.84$ rad partial reflection of the electromagnetic wave would occur (i.e. reflection of the ordinary wave component) due to the ordinary mode being in the second stop band; the fast extraordinary (FE) is in the pass band.

Figure 4 illustrates a graphical method for determination of the critical angles of incidence θ_{in} (Bragg), the region of propagation considered being that of O and SE. For the ordinary wave, curve 'O' is plotted by determining $\sin \theta_{in}$ (left hand

Table 2

Critical angles of Bragg reflection for a given ω_c/ω_p and ω/ω_p in a low and high density plasma.

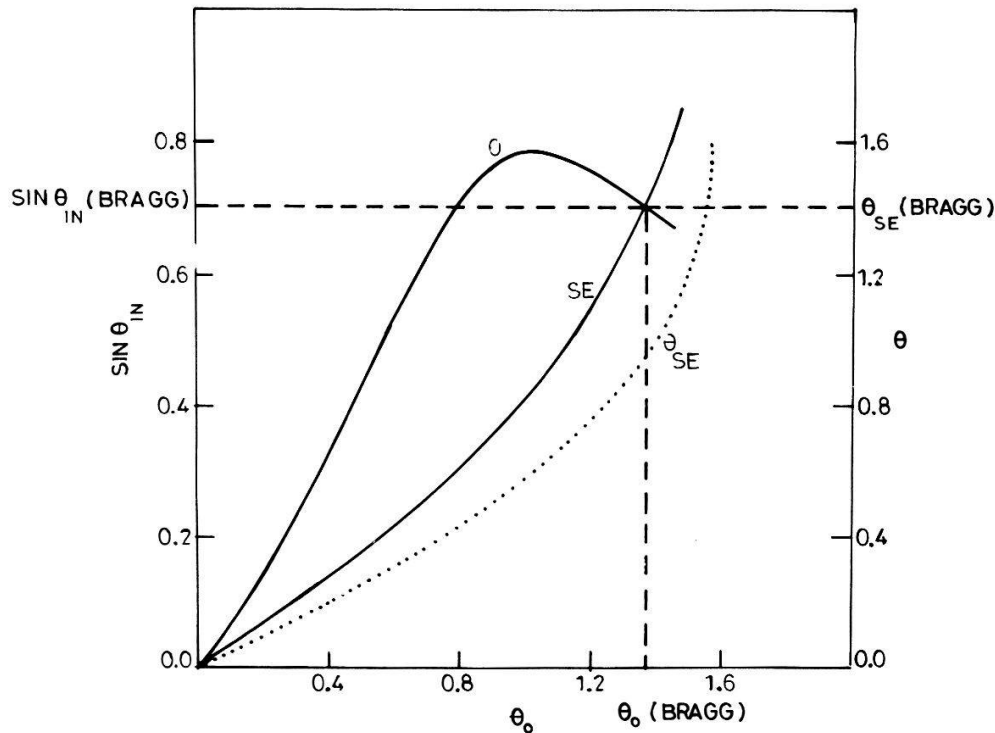| $\dfrac{\omega_c}{\omega_p}$	$\dfrac{\omega}{\omega_p}$	Modes (1, 2)	a_1, a_2	θ_B	θ_1, θ_2	θ_{in} (Bragg)
				In radians		
0.00136	1.006	O, FE	3.92	0.052	1.54	
			278.15		1.34	0.097
0.1	1.07	O, FE	4.0	0.136	1.55	
			678.6		1.42	0.84
9.525	10.35	O, FE	9.04	2.846	1.53	
			262.49		1.33	1.35
10.0	1.4	O, SE	1.01	0.728	1.44	
			379.15		0.922	0.964
29.8	30.1	O, FE	4.0	2.772	1.54	
			241.24		1.32	1.37
30.0	1.15	O, SE	1.09	0.785	1.36	
			25.62		0.76	0.78

Figure 4
θ_{SE} to be read off from right hand ordinate is calculated from first order Bragg condition (Equation (13a) with $m = 1$) for given θ_O (abscissa). The lefthand ordinate is $\sin \theta_{in}$ calculated using Snell's law (Equation (13b)) on θ_O and θ_{SE}. The ordinary wave is in the first stop band for Bragg reflection (partial) of the wave incident from vacuum. Plasma parameters are: $\omega/\omega_p = 1.15$; $\omega_c/\omega_p = 30$.

ordinate) from Snell's law (equation (14b)) assuming θ_0 to be given. For the slow extraordinary wave, a plot of θ_{SE} (shown as the right hand ordinate) *Vs* θ_O is given where θ_{SE} is determined from the Bragg condition for the given θ_O. Finally, with known θ_{SE}, Snell's law for the extraordinary wave is used to obtain the values of $\sin \theta_{in}$ again and the curve labelled SE is plotted. Clearly, only at the intersection points of the curves O and SE, Snell's law for both the waves as well as the Bragg condition for the O wave are self-consistent. The point at the origin represents normal incidence ($\theta_{in} = 0$). It implies that at normal incidence Bragg reflection is always possible if the parameters are properly adjusted. The second point θ_{in} (Bragg) is the critical angle of incidence around which the O wave is reflected. The critical angle hence determined has been found to agree closely with the value determined numerically.

Figure 4 above considers first order ($m = 1$) Bragg reflection. Higher order Bragg reflections would be less accessible because of narrower windows of parameters like ω and higher thresholds. Further, while NBR can be total for normal incidence as both the modes are in the stop bands simultaneously, for oblique incidence it is partial because only one of the modes can be in the stop band, the modes being non-collinear.

Observability of NBR

Nonlinear Bragg reflection would be observable when the power of the incident electromagnetic wave scattered from the zero frequency modulation

exceeds the incoherent scattering from the background thermal fluctuations. Otherwise this phenomenon has apparently no threshold in contrast to parametric scattering processes like stimulated Brillouin scattering (SBS) or stimulated Raman scattering (SRS). In a low collisional plasma, however, the observability thresholds of NBR and SBS/SRS could be comparable since the existence thresholds of the latter processes are small enough, and the observability depends mainly on the noise levels at the appropriate frequency shifted lines. The NBR line with zero frequency shift (in the absence of the usually present plasma drifts) could, in principle, be less noisy than SBS or SRS lines which support noise levels of the natural modes of the plasma. In practice, on account of the presence of drifts (28) and cascading, the 'zero frequency' noise levels could, however be high enough to compare with that of the SBS/SRS lines.

To determine the required power for detection of NBR, the average thermal density fluctuation of an equilibrium plasma may be substituted in the equation for the density modulation (equation (6c)) to obtain normalised power $E^2/8\pi n_0 T_e$. For instance, in quiescent laboratory plasmas characterised by $\delta n/n \lesssim 0.1\%$, the (normalised) pump power should be greater than 10^{-2}; this falls in the intermediate/strong range of microwave power. Specifically, (for example) $\delta n/n = 0.17\%$ in the high frequency regime with the parameters $\omega_c/\omega_p = 0.1$, $\omega/\omega_p = 1.051$, $\theta_B = 45°$ where the normal waves in the stop bands are O and FE; in a low density plasma with $\omega_c/\omega_p = 50$ and $\theta_B = 45°$, $\delta n/n = (0.1\%, 0.01\%, 0.31\%)$ are created at ω/ω_p (50.04, 1.01, 0.019) in the stop bands of (O, FE), (O, SE) and (SE, FMS) respectively. The above values could be an overestimate since the actual thermal fluctuation at zero frequency would be much less than the average value as the principal contribution to the latter comes from the peak at the ion line ($\omega_c/\omega_p \ll 1$) when $T_e \gg T_i$ (and neglecting turbulence effects). Consequently the Bragg scattered wave may be detectable below the above threshold (even though the frequency shifted scattering due to the ion line may be more intense). For ionosphere, a similar estimate is $E^2/8\pi n_0 T_e \geq 10^{-3}$, the thermal $\delta n/n$ being 0.01% ($n = 10^6$ particles/cm^3 $T = 1$ eV).

It is interesting to compare the zero frequency modulation level with the saturated values of $\delta n_i/n$ (of ions) measured in laser plasma interaction during SBS. For instance at strong pump powers of $E^2/8\pi n_0 T_e \simeq 1$ (Intensity 10^{12} Watt/cm^2 for Nd glass lasers) when the SBS reflectivity is 20%, the observed $\delta n_i/n \simeq 10\%$ (28); the zero frequency modulation is also of the same order at these powers (10^4 times the thermal value). One may, therefore, expect NBR to compete with SBS in laser plasma interaction. (It should be detectable at a shifted frequency corresponding to the drift of the underdense plasma; this process is different from the case of magnetoplasma in that the modulation is created by the beating of the incident wave and the reflected wave from the critical density region (22)).

In a more complete analysis, drifts due to inhomogneties should be considered as these are unavoidable in a magnetoplasma. In such a case, the Doppler shift in the reflected wave and hence the modulation would enable a resonant coupling to a normal mode such as the universal drift mode in a low β plasma (which satisfies $\omega = \frac{1}{2}(K_\perp V_D \pm (K_\perp^2 V_D^2 + 4K_\parallel^2 C_S^2)^{1/2})$. Hence, NBR would

be observable when the modulation created by the wave exceeds the fairly large fluctuation level of the drift mode which is always present in an inhomogeneous plasma. Typical values of $\delta n/n$ of drift waves for example in a Q-machine, are about 5–6% (29) which is much higher than the thermal level; normalised pump powers of about 0.1 may then be required for detection of NBR. At these powers, parametric instabilities may also be excited. While, the Bragg scattered wave can be enhanced if the reflected and the drift wave grow at the expense of the incident wave, other parametric instabilities like decay instabilities may drain energy from the electromagnetic waves (by coupling to other normal modes) and compete with NBR, since the observability thresholds are comparable.

5. Summary and conclusions

We have investigated a new ponderomotive effect for uniform plane electromagnetic waves in a cold magnetoplasma in situations where different polarisation components of the same wave with different wave numbers but same frequency, beat to produce a spatially periodic modulation of the magnetoplasma. This modulation leads to Bragg reflection of the incident wave because of the appearance of the stop bands in the wave characteristics. For normal incidence when both the waves are in the stop bands, total reflection occurs while partial reflection occurs for oblique incidence when only one of the modes is in the stop band. For weak nonlinearity and absorption, this would occur at all powers and does not need a threshold. However, to be distinguishable from other incoherent scattering due to thermal fluctuations, power levels comparable to SBS are necessary when the density fluctuation level due to the wave is raised above the thermal noise. The Bragg condition for reflection for oblique incidence gives certain critical angles of incidence while for normal incidence reflection occurs in certain frequency band gaps for given plasma parameters ω_p, ω_c.

One may venture to conclude that the stop bands should be avoided in wave heating of plasmas as enhanced reflection of the wave would occur. The stop bands are, however, useful for enhanced reflection e.g. from the ionosphere in radiowave communication. The use of pass bands as an efficient channel for dumping wave energy by cyclotron damping or drift wave excitation would be taken up elsewhere [22].

While this study should be considered as a preliminary indication of the new ponderomotive effects, further elaboration of the processes including the effects of self consistency, geometry, finiteness and inhomogeneity would be necessary to be able to relate better to realistic actual experiments and are likely to be dealt with in a future communication.

REFERENCES

[1] P. M. BELLAN and J. ADAM in *Laser Plasma Interaction*, (Stern Verlag, Dusseldorf, 1983).
[2] MIKLOS PORKOLAB in *Fusion* ed. Edward Teller, (Academic Press, New York, 1981).
[3] S. HIROE, T. SATO *et al.*, Phys. Fluids *21*, 676, (1978).
[4] PHILLIPPE L. SIMILON and A. N. KAUFMAN, Phys. Rev. Lett. *53*, 1061, (1984).
[5] A. V. GUREVICH in *Nonlinear Phenomena in Ionosphere*, (Springer, New York, 1978).
[6] M. N. ROSENBLUTH and R. Z. SAGDEEV in *Handbook of Plasma Physics*, Vols. 1 and 2., (North Holland Physics Publishing, New York, 1984).
[7] D. SUBBARAO, R. UMA and A. K. GHATAK, Laser and Particle Beams, *1*, 367, (1983).
[8] R. W. SHORT and E. A. WILLIAMS, Phys. Rev. Lett. *47*, 337, (1981).
[9] S. G. THORNHILL and D. TER HAAR, Phys. Reports *43*, 43, (1978).
[10] J. A. STAMPER, Phys. Fluids *15*, 735 (1975).
[11] H. MOTZ and C. J. WATSON, 67, Advances in Electronics and Electron. Phys. 23, 153.
[12] E. S. WEIBEL and M. C. FESTEAU-BARRIOZ, Pl. Phys., *24*, 243 (1982).
[13] L. P. PITAEVSKII, Soviet Phys. JETP, *12*, 1008 (1961).
[14] V. I. KARPMANN and A. G. SHAGALOV, Jl. Plasma Phys. *27*, 215 (1982).
[15] J. R. CARY and A. N. KAUFMAN, Phys. Fluids, *24*, 1238 (1981).
[16] G. STATHAM and D. TER HAAR, Plasma Phys. *25*, 681 (1983).
[17] D. SUBBARAO (1981) Report: IIT Delhi/CES/FUS.
[18] R. UMA and D. SUBBARAO, Phys. Lett., *106A*, 423 (1984).
[19] A. N. KAUFMAN, J. R. CARY and N. R. PEREIRA, Phys. Fluids, *22*, 790 (1979).
[20] L. D. LANDAU and E. M. LIFSHITZ in *Electrodynamics of continuous media*, (Pergamon Press and Addison Wesley, 1960).
[21] K. C. YEH and C. H. LIU in *Ionospheric Waves*, (Academic New York, 1972).
[22] R. UMA and D. SUBBARAO (1983) Report: IIT Delhi/CES/FUS.
[23] N. W. MCLACHLAN in *Theory and Applications of Mathieu Functions*, (Dover Publications, New York, 1964).
[24] LEON BRILLOUIN in *Wave Propagation in Periodic Structures*, (Mcgraw Hill, New York, 1946).
[25] T. TAMIR, H. E. WANG, and A. A. OLINER, IEEE Trans, Microwave Theory Tech., MTT-12, 324, (1964). Charles Elechi, Proc. IEEE, *64*, 1666 (1976).
[26] P. K. KAW, A. T. LIN and J. M. DAWSON, Phys. Fluids, *16*, 1967 (1973).
[27] B. COHEN, A. N. KAUFMAN and K. WATSON, Phys. Rev. Lett. *29*, 581 (1972).
[28] P. BROSSIER, P. DESCHAMPS, R. GRAVIER, R. PELLAT and C. RENAUD, Phys. Rev. Lett., *26*, 124 (1971).
[29] R. GILES and A. A. OFFENBERGER, Phys. Rev. Lett. *50*, 421, (1983).